

## In-plane anisotropy in the microwave dielectric properties of SrTiO<sub>3</sub> films

Wontae Chang, Steven W. Kirchoefer, Jeffrey A. Bellotti, Syed B. Qadri, Jeffrey M. Pond, Jeffrey H. Haeni, and Darrell G. Schlom

Citation: *Journal of Applied Physics* **98**, 024107 (2005); doi: 10.1063/1.1984074

View online: <http://dx.doi.org/10.1063/1.1984074>

View Table of Contents: <http://scitation.aip.org/content/aip/journal/jap/98/2?ver=pdfcov>

Published by the [AIP Publishing](#)

---

### Articles you may be interested in

Enhanced microwave dielectric tunability of Ba<sub>0.5</sub>Sr<sub>0.5</sub>TiO<sub>3</sub> thin films grown with reduced strain on DyScO<sub>3</sub> substrates by three-step technique

*J. Appl. Phys.* **113**, 044108 (2013); 10.1063/1.4789008

In-plane microwave dielectric properties of paraelectric barium strontium titanate thin films with anisotropic epitaxy

*Appl. Phys. Lett.* **87**, 082906 (2005); 10.1063/1.2031938

Effect of anisotropic in-plane strains on phase states and dielectric properties of epitaxial ferroelectric thin films

*Appl. Phys. Lett.* **86**, 052903 (2005); 10.1063/1.1855389

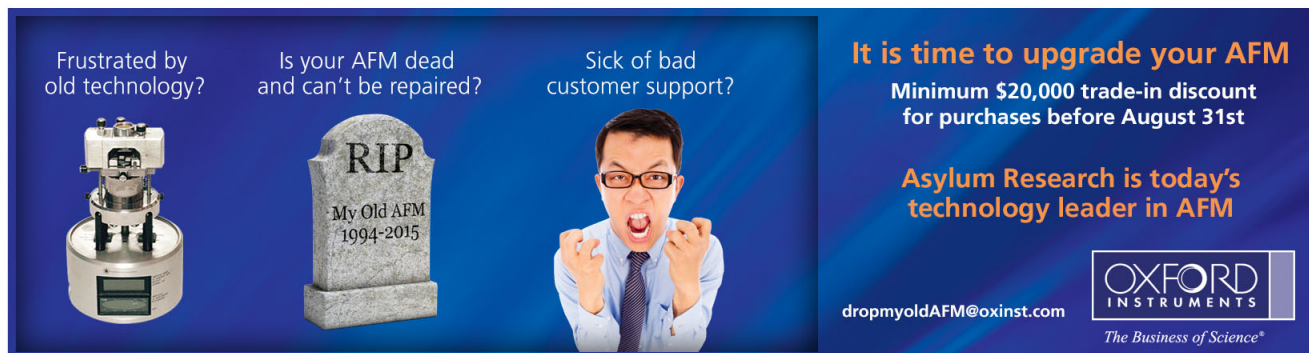
Effects of buffer layer thickness and strain on the dielectric properties of epitaxial SrTiO<sub>3</sub> thin films

*J. Appl. Phys.* **92**, 6149 (2002); 10.1063/1.1515100

Microstructure and microwave dielectric properties of epitaxial SrTiO<sub>3</sub> films on LaAlO<sub>3</sub> substrates

*J. Appl. Phys.* **83**, 4884 (1998); 10.1063/1.367288

---



Frustrated by old technology? Is your AFM dead and can't be repaired? Sick of bad customer support?

**It is time to upgrade your AFM**

Minimum \$20,000 trade-in discount for purchases before August 31st

Asylum Research is today's technology leader in AFM

dropmyoldAFM@oxinst.com

**OXFORD INSTRUMENTS**  
The Business of Science®

# In-plane anisotropy in the microwave dielectric properties of SrTiO<sub>3</sub> films

Wontae Chang,<sup>a)</sup> Steven W. Kirchoefer, Jeffrey A. Bellotti, Syed B. Qadri, and Jeffrey M. Pond

Naval Research Laboratory, Washington, D.C. 20375

Jeffrey H. Haeni and Darrell G. Schlom

Pennsylvania State University, University Park, Pennsylvania 16802

(Received 23 November 2004; accepted 29 May 2005; published online 22 July 2005)

Microwave tunable dielectric properties of strained (001) SrTiO<sub>3</sub> thin films epitaxially deposited on (110) DyScO<sub>3</sub> substrates were studied for in-plane film orientations ([100], [010], [110], and [-110]). A significant in-plane anisotropy in dielectric constant and tuning was observed in these SrTiO<sub>3</sub> films. The highest dielectric constant and tuning at room temperature are observed along the [010] direction of the SrTiO<sub>3</sub> film (1000 Å thick) (3500 and 70% at 1 V/μm, respectively), the lowest ones are observed along the [100] direction (i.e., 2000 and 50% at 1 V/μm, respectively). The dielectric constant and tuning along [-110] and [110] are about 2500 and 30% at 1 V/μm, respectively, which are intermediary to those along the [010] and [100] directions. The dielectric  $Q(=1/\tan \delta)$  does not show any large difference for the four directions (i.e.,  $Q \sim 10-20$ ). Also, the phase-transition peak for the [-110] and [110] directions of the SrTiO<sub>3</sub> film (300 Å thick) is observed at 275 K, which is lower than that for the [010] and [100] directions. The observed in-plane anisotropic dielectric properties have been interpreted based on the phenomenological thermodynamics of film strain.

## I. INTRODUCTION

SrTiO<sub>3</sub> is known as an incipient ferroelectric material, whose ferroelectric phase transition is suppressed by quantum fluctuations and whose nonlinear dielectric properties are exhibited only at very low temperatures (i.e., below 65 K).<sup>1-3</sup> Recently, it has been demonstrated that SrTiO<sub>3</sub> thin films (500 Å thick) epitaxially grown on (110) DyScO<sub>3</sub> substrates using molecular-beam epitaxy (MBE) were extremely strained (~1% in-plane tensional strain) from 3.905 Å of bulk SrTiO<sub>3</sub>, and the room-temperature in-plane dielectric constant and its tuning of the films at 10 GHz were observed to be 6000 and 75% with an electric field of 1 V/μm, respectively.<sup>4,5</sup> The control of strain in SrTiO<sub>3</sub> provides a basis for room-temperature tunable microwave applications by elevating its phase-transition peak to room temperature, resulting in large dielectric constants and dielectric tuning at 300 K.

In ferroelectric thin films, polarization mechanisms in both ferroelectric and paraelectric phases are significantly different from those in the corresponding bulk materials mainly because films are strained and clamped by substrates, resulting in a structural phase distortion (i.e., structural symmetry changes). The modification of structural symmetry in films determines the relevant polarization formations in terms of its magnitude and direction, and its motion with applied electric fields.<sup>6,7</sup> Subsequently, such structural distortions of ferroelectric thin films caused by film strain have a strong impact on the microwave dielectric properties. For example, it was reported that film strains, both biaxial compression and biaxial tension, shift the paraelectric to ferroelectric phase-transition peak to higher temperatures.<sup>6</sup> The

increase in-phase-transition temperature is a result of tensional film strain in both cases (i.e., biaxial compression and biaxial tension) because the relevant ferroelectric polarization forms along the direction of tensional strain (i.e., a tensile strain field occurs normal or parallel to the film surface for biaxially compressed or biaxially extended films, respectively), which causes the phase-transition temperature to increase. However, this does not necessarily mean that the ferroelectric polarization always forms only along the direction of tensional strain in films (i.e., normal to the film surface for biaxially compressed films or parallel to the film surface for biaxially extended films), although it is likely to occur that way in most films. In other words, the ferroelectric polarization can form in a direction of compressed strain field if the total film energy can be minimized by doing so, and in such cases, the phase-transition temperature can be expected to decrease. Therefore, the experimental measurement direction becomes very important, especially in the case of a directionally well-oriented film. For example, if the measurement direction is in-plane of the biaxially compressed ferroelectric film and if its polarization forms along the normal direction of the film surface, we may miss significant effects caused by the phase transition. In this article, the film structure and the directional microwave dielectric properties for highly strained SrTiO<sub>3</sub> films deposited on (110) DyScO<sub>3</sub> single-crystal substrate are characterized and analyzed for the in-plane film orientations [-110], [010], [110], and [100].

## II. EXPERIMENT

SrTiO<sub>3</sub> thin films (300 and 1000 Å thick) have been deposited onto (110) DyScO<sub>3</sub> single-crystal substrates at 650 °C by molecular-beam epitaxy.<sup>4,8</sup> The films were an-

<sup>a)</sup>Electronic mail: chang@estd.nrl.navy.mil

nealed for 30 min at 700 °C in atmosphere to reduce the oxygen vacancies, which might form during the film deposition. The DyScO<sub>3</sub> crystal substrate is an LnMO<sub>3</sub> orthorhombic structure (Pbnm)<sup>9,10</sup> with anisotropic dielectric properties.<sup>11</sup> The lattice parameters  $a_1$ ,  $a_2$ , and  $a_3$  are 5.440, 5.713, and 7.887 Å, respectively, and the dielectric constants  $\epsilon_1$ ,  $\epsilon_2$ , and  $\epsilon_3$  are 22.0, 18.8, and 35.5, respectively. The deposited SrTiO<sub>3</sub> films are extremely strained (i.e., ~1% in-plane tensional strain) but still exhibit a high degree of uniformity and structural perfection resulting from an extremely small lattice mismatch (~1%) with (110) DyScO<sub>3</sub> single-crystal substrates and a well-controlled layer-by-layer film growth using reactive molecular-beam epitaxy (MBE).<sup>4,8</sup> Detailed information on film deposition can be found in the references.<sup>4,8</sup> X-ray diffraction (XRD) was used for in-plane substrate orientation and film structure characterization.

Interdigitated capacitors (IDC) were deposited on top of the SrTiO<sub>3</sub> films (300 and 1000 Å thick) through a polymethylmethacrylate (PMMA) lift-off mask by e-beam evaporation of 1.5- $\mu$ m-thick Ag with an adhesive thin layer of Cr and a protective thin layer of Au. The microwave dielectric properties, capacitance and device  $Q$  of SrTiO<sub>3</sub> thin films, were measured as a function of frequency (45 MHz to 20 GHz), dc bias voltage (-40–40 V), temperature (10–330 K), and in-plane film orientation (0°, 45°, 90°, and 135°, with respect to [112] DyScO<sub>3</sub>).  $S_{11}$  measurements were made on these interdigitated capacitors by probing with a 200- $\mu$ m pitch Picoprobe microwave probe connected to an HP 8510C network analyzer. The measured  $S_{11}$  data were fitted to a parallel resistor-capacitor model to determine the capacitance and device  $Q$  of the films. The dielectric constant of the films was extracted from the device capacitance and the IDC capacitor dimensions through a conformal mapping technique.<sup>12</sup>

### III. RESULTS AND DISCUSSION

#### A. Film and substrate structures

The in-plane orientation of (110) DyScO<sub>3</sub> single-crystal substrates used in this research was characterized first because DyScO<sub>3</sub> crystal substrate is an LnMO<sub>3</sub> orthorhombic structure (Pbnm)<sup>9,10</sup> with anisotropic dielectric properties.<sup>11</sup> Figure 1 shows XRD patterns of DyScO<sub>3</sub> substrate in-plane orientations: (a) 0°, (b) 45°, (c) 90°, and (d) 135°. The inset in Fig. 1(a) describes the orientation with respect to the substrate. Unlike what was expected, the 0° and 90° in-plane orientations in the (110) DyScO<sub>3</sub> substrates used in this research are (112) and (11-2) planes, respectively, and the 45° and 135° orientations are the (110) and (001) planes, respectively, as shown in Fig. 1. Therefore, the edges of the substrates are parallel to and perpendicular to [112] DyScO<sub>3</sub>, and the 45° and 135° directions of the substrates are the [110] and [001] DyScO<sub>3</sub>, respectively.

Figure 2 shows XRD patterns of asymmetric (024) peaks of SrTiO<sub>3</sub> thin film (1000 Å thick) deposited onto the (110) DyScO<sub>3</sub> single-crystal substrate. It is worth noting that the asymmetric SrTiO<sub>3</sub> (024) reflections were obtained only after the substrate was rotated by 45° and 135° in the substrate

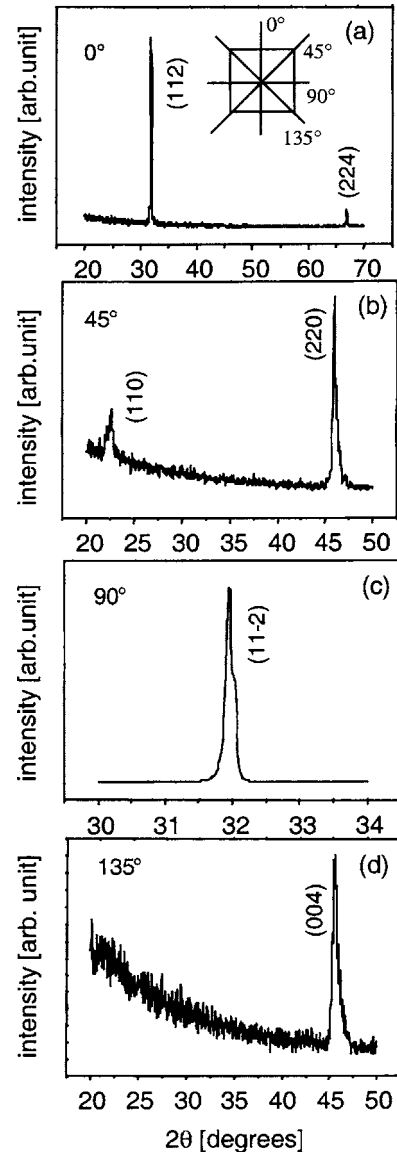


FIG. 1. XRD patterns of DyScO<sub>3</sub> substrate in-plane orientations: (a) 0°, (b) 45°, (c) 90°, and (d) 135°.

plane with respect to the substrate edge, indicating that the edge of the SrTiO<sub>3</sub> unit cell is rotated 45° and 135° from the substrate edge. Also, the diffraction pattern for asymmetric (024) reflections was obtained from a monochromatic x-ray source ( $K\alpha_1$  only) generated using a Ge(111) crystal. The

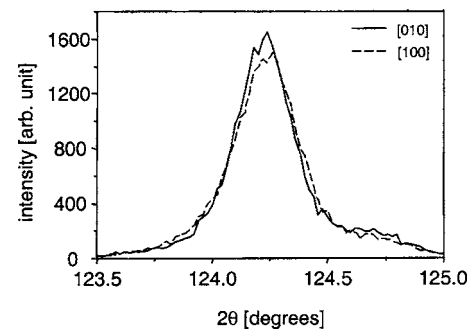


FIG. 2. XRD patterns of asymmetric (024) peaks of SrTiO<sub>3</sub> thin film (1000 Å thick) with 45° and 135° rotation with respect to [112] DyScO<sub>3</sub>.

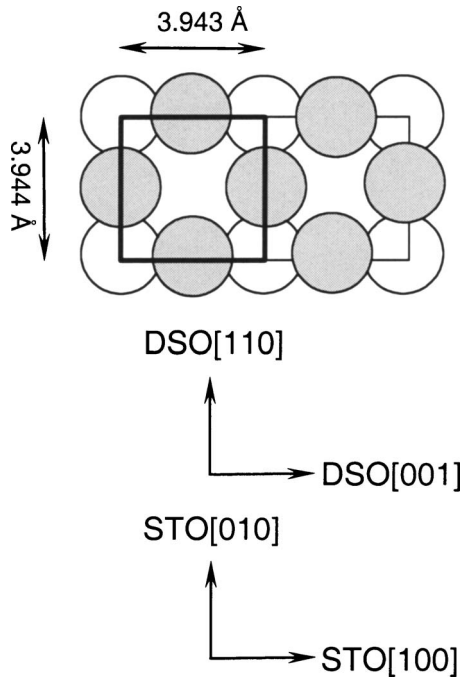


FIG. 3. Possible oxygen adsorption sites (gray circles) for SrTiO<sub>3</sub> film on (110) DyScO<sub>3</sub> substrate (the white circles are substrate oxygen atoms).

lattice parameters in the plane of the film ( $a_{\parallel}$ ) along the 45° and 135° directions, which are denoted as [010] SrTiO<sub>3</sub> and [100] SrTiO<sub>3</sub> in this paper, respectively, were determined from the XRD patterns of asymmetric (024) reflections (Figs. 2 and 3) by fitting with a Gaussian function after removing the background. The determined in-plane lattice parameters  $a_1$  and  $a_2$  of SrTiO<sub>3</sub> film (1000 Å thick) are 3.941 and 3.942 Å, respectively, which are nearly identical within a measurement error ( $< \pm 0.001$  Å). It is worth noting that the measurement error is mostly due to an instrumental error (i.e., a systematic error) and not from an uncertainty in the fitting procedure to determine the peak position. Therefore, the SrTiO<sub>3</sub> film unit cell is biaxially strained, with the magnitude of strain in the [100] and [010] directions being approximately but not being identically equal, in which both in-plane parameters,  $a_1$  and  $a_2$ , are severely strained ( $\sim 1\%$  of tension) from the corresponding bulk lattice parameter (3.905 Å).

To understand how the SrTiO<sub>3</sub> films deposited on the (110) DyScO<sub>3</sub> are strained to this extent, we examined how the atoms in SrTiO<sub>3</sub> structure could adsorb on the substrate. Based on the DyScO<sub>3</sub> crystal symmetry (Pbnm) and the XRD patterns of (001) SrTiO<sub>3</sub> films on the (110) DyScO<sub>3</sub> substrate, possible adsorption sites of the film oxygen atoms can be presumed as shown in Fig. 3. The strontium atoms could sit on top of the substrate oxygen atoms (white circles) and, in the subsequent layer, the film oxygen atoms (gray circles) and titanium atoms could sit between two neighboring strontium atoms, and at the center of the four film oxygen atoms, respectively. Consequently, the possible in-plane unit-cell size of the SrTiO<sub>3</sub> film is a  $3.943 \times 3.944$  Å which is commensurate with the pseudocubic (110) DyScO<sub>3</sub> substrate. These values are very close to the measured lattice parameter of SrTiO<sub>3</sub> films (i.e., 3.941 and 3.942 Å). This

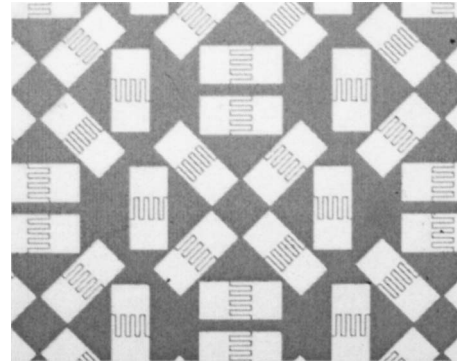


FIG. 4. Interdigitated electrodes deposited on top of SrTiO<sub>3</sub> thin films for the directional dielectric measurements (gap size = 8 μm, finger width = 10 μm, finger length = 80 μm).

indicates that the observed strains are mostly due to the lattice mismatch between the film and the substrate. Also, the reason the in-plane parameters  $a_1$  and  $a_2$  of the SrTiO<sub>3</sub> film can be slightly different from each other is the pseudocubic in-plane unit-cell size of the (110) DyScO<sub>3</sub> substrate ( $3.943 \times 3.944$  Å).

## B. Microwave dielectric properties: Experimental measurements

A study of directional dielectric properties of SrTiO<sub>3</sub> films (300 and 1000 Å thick) was made in the directions of [100], [010], [110], and  $[-110]$  of the SrTiO<sub>3</sub> films. Figure 4 shows the interdigitated electrodes deposited on top of the SrTiO<sub>3</sub> thin films for the directional dielectric measurements (gap size = 8 μm, finger width = 10 μm, finger length = 80 μm). We have been careful to minimize effects, such as film thickness and electrode dimension variations, which cause erroneous extraction of the relative permittivity values by using only closely spaced, precisely defined, interdigitated electrodes as shown in Fig. 4.

Figure 5 shows the room-temperature dielectric constant of the annealed 1000-Å-thick SrTiO<sub>3</sub> film as a function of applied dc bias voltages for the four different directions described previously. As shown in Fig. 5, no significant difference is observed in the dielectric constant and tuning between the [110] and  $[-110]$  directions of the SrTiO<sub>3</sub> film ( $\sim 2500$  and 30% at 1 V/μm, respectively), but there is a significant difference in those dielectric properties between the [100] and [010] directions. The dielectric constant and tuning along the [010] direction are observed to possess the

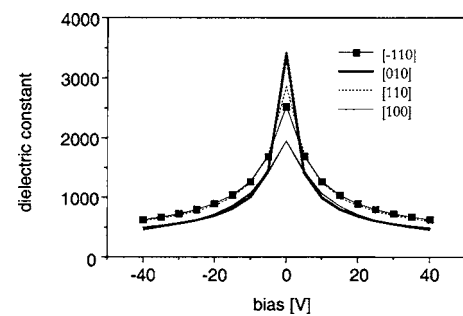


FIG. 5. Directional dielectric constant of SrTiO<sub>3</sub> thin film (1000 Å thick) as a function of dc bias voltages at 10 GHz and at room temperature.

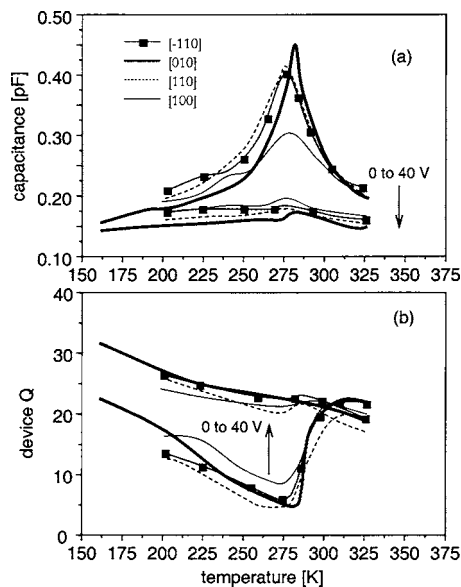


FIG. 6. Directional (a) capacitance and (b) device  $Q$  of SrTiO<sub>3</sub> thin film (300 Å thick) as a function of temperature and dc bias voltages at 10 GHz.

highest values (3500 and 70% at 1 V/ $\mu$ m, respectively), and those along the [100] direction exhibit the lowest ones (2000 and 50% at 1 V/ $\mu$ m, respectively). This trend in the directional property is typical to a greater or lesser extent for all other films  $\geq 200$  Å thick. These observations of in-plane dielectric property anisotropies can be explained by breaking the in-plane film structure symmetry induced by the film strain, which can subsequently determine the electric polarization (i.e., magnitude and direction) in the film. The [110] and [-110] directions of the SrTiO<sub>3</sub> film have no difference in terms of structural symmetry and film strain, which naturally results in having no difference in the dielectric constant and tuning in these directions. However, the [100] and [010] directions of the film, which show a significant difference in the film strain ( $a_1=3.941$  Å and  $a_2=3.942$  Å), even though the difference between the in-plane film strains is extremely small ( $x_1$  and  $x_2$  are 0.0092 and 0.0094, respectively), which significantly affects the paraelectric phase polarization at room temperature as seen in the measurements. This is because the magnitude of paraelectric ionic polarization (induced by applied electric field) could be larger in [010] SrTiO<sub>3</sub> than [100] SrTiO<sub>3</sub> from the strain difference. Also, in the ferroelectric phase, the slight difference in film strain is expected to cause the direction of ferroelectric spontaneous polarization (i.e., tetragonal ferroelectric phase) to be more probable in the [010] direction in SrTiO<sub>3</sub> rather than in the [100] SrTiO<sub>3</sub>. Consequently, the dielectric constant and tuning in the [010] direction of the SrTiO<sub>3</sub> film (which is parallel to [001] DyScO<sub>3</sub>) must be larger than those in the [100] direction of the SrTiO<sub>3</sub> film, consistent with the tensional strain being larger in the [010] direction than in the [100] direction.<sup>13</sup>

Figure 6 shows the directional capacitance and device  $Q$  of a 300-Å-thick SrTiO<sub>3</sub> thin film as a function of temperature and dc bias voltages at 10 GHz. The temperature-dependent capacitance measurements of the SrTiO<sub>3</sub> film

show that the phase-transition peaks from all the four directions are elevated to just below room temperature. Also, it is observed that the phase-transition peak in the [100] and [010] directions of the SrTiO<sub>3</sub> film shows a significant difference in terms of peak height and peak width (i.e., the peak along the [010] direction is higher and sharper than that along the [100] direction). In comparison, the capacitance in the [110] and [-110] directions displays almost the same temperature dependence, where the phase-transition temperature is about 275 K, which is 5 K lower than that of the [010] direction. The phase transition along the [100] direction shows the broadest peak, which is between the peak of the [110] and [-110] directions ( $\sim 275$  K) and the peak of the [010] direction ( $\sim 280$  K). These temperature- and directional-dependent observations on the phase transition of the film [Fig. 6(a)] are consistent with room-temperature measurements (Fig. 5) and explain why the dielectric constant and tuning at room temperature depend on the measurement directions (Fig. 5). However, it is very interesting to observe that the phase-transition peak can be different depending on the measurement direction because traditionally the transition temperature has been treated as a scalar quantity. Figure 6(b) shows that the directional-dependent device  $Q$  of the SrTiO<sub>3</sub> films does not show any technically important difference, having a typical device  $Q$  ( $\sim 10$ ) at 0-V dc bias at 275 K, which is associated with the phase-transition peak. The device  $Q$ 's of the films, which look too low to be applied to real devices, is believed to be mostly due to the dielectric  $Q$  ( $=1/\tan \delta$ ) because any other loss factors (i.e., electrode resistance, leakage current, and substrate dielectric) are expected to be much lower compared to the dielectric loss in the film. A series capacitor-resistor model does not fit the experimental data, so parasitic loss mechanisms best modeled by series components are not significant. Since the primary loss mechanism is expected to be due to the dielectric loss tangent of the ferroelectric, the device is modeled as a bias-dependent ideal capacitor parallel with a bias-dependent and frequency-dependent resistance that best fits the data.<sup>14</sup> It is also worth noting that, in Fig. 6(b), the dc bias dependence of the device  $Q$  ( $=1/\tan \delta$ ) of the SrTiO<sub>3</sub> thin film (300 Å thick) changes at a region of the paraelectric phase close to the phase-transition peak. Below this region (i.e., ferroelectric phase) the device  $Q$  increases with dc bias, and above this region (i.e., paraelectric phase) the  $Q$  decreases with dc bias. We observed this kind of  $Q$  dependencies with dc bias in other films [i.e., (Ba,Sr)TiO<sub>3</sub> films on MgO or LaAlO<sub>3</sub> substrate] at the same region of the paraelectric phase around the phase-transition peak in our previous research work. A further study on this observation is necessary to clarify the involved loss mechanism(s) around the phase-transition peak.

### C. Microwave dielectric properties: Theoretical analysis

The reason why the dielectric constant and the phase-transition peak of the SrTiO<sub>3</sub> films depend on the direction of the applied small-signal electric field can be explained based on Devonshire's phenomenological theory.<sup>15</sup> Previously, we

reported a theoretical analysis of the dielectric properties of epitaxial (Ba, Sr)TiO<sub>3</sub> and SrTiO<sub>3</sub> films based on the thermodynamic theory to explain the film strain effect on the dielectric constant, dielectric tuning, and phase-transition peak.<sup>5,13</sup> The theoretical expression between the strain-induced phase-transition peak  $T_C^*$  and the film strain  $x$  (i.e., in-plane strain for our measurement configuration) can be expressed as

$$T_C^* = T_C - 2\varepsilon_0 C \{G_{11}x_1 + G_{12}(x_2 + x_3)\}, \quad (1)$$

where  $T_C$  is the phase-transition temperature of SrTiO<sub>3</sub> with no strain. The relevant parameters in this expression, used throughout this article, can be found elsewhere.<sup>5,16-19</sup> Equation (1) is applicable only to the case of the applied small-signal electric field parallel to the [100] direction of the SrTiO<sub>3</sub> film (i.e., parallel to the in-plane film strain  $x_1$ ), that is, the field-induced polarization forms only in the same direction (i.e.,  $P_1$  or  $P_{[100]}$ ). Similarly, the corresponding expression for the case of the applied electric field parallel to the [010] direction of the SrTiO<sub>3</sub> film can be expressed simply by switching the in-plane strains  $x_1$  and  $x_2$  in the above expression as

$$T_C^* = T_C - 2\varepsilon_0 C \{G_{11}x_2 + G_{12}(x_1 + x_3)\}. \quad (2)$$

Now, to get the expression for the case of the electric field parallel to the [110] or [-110] direction of the SrTiO<sub>3</sub> films, we take the same procedure as in the previous case starting from the Gibbs free energy from the theory,<sup>15</sup>

$$G(T, P_i, X_j) = F(T, P_i, x_j) - E_i P_i, \quad (3)$$

where  $F(T, P_i, x_j)$ , the Helmholtz free energy, can be expressed as  $F_0 + 1/2\alpha(P_1^2 + P_2^2 + P_3^2) + 1/4\beta(P_1^4 + P_2^4 + P_3^4) + 1/6\gamma(P_1^6 + P_2^6 + P_3^6) + 1/2\delta(P_2^2 P_3^2 + P_3^2 P_1^2 + P_1^2 P_2^2) + 1/2c_{11}(x_1^2 + x_2^2 + x_3^2) + c_{12}(x_2 x_3 + x_3 x_1 + x_1 x_2) + 1/2c_{44}(x_1^2 + x_2^2 + x_3^2) + G_{11}(x_1 \times P_1^2 + x_2 P_2^2 + x_3 P_3^2) + G_{12}\{x_1(P_2^2 + P_3^2) + x_2(P_3^2 + P_1^2) + x_3(P_1^2 + P_2^2)\} + G_{44}(x_4 P_2 P_3 + x_5 P_3 P_1 + x_6 P_1 P_2) + \dots$ . Then, the nonlinear relationship between polarization and electric field can be obtained by minimizing the Gibbs free energy  $G$  with respect to the polarization  $P$  because  $G$  must be a minimum for a stable state of the ferroelectric at a constant temperature,

$$\partial G / \partial P_i = \partial F / \partial P_i - E_i = 0. \quad (4)$$

To perform this equation for the small-signal electric field parallel to the [110] and [-110] directions of the film, we assume that the applied electric field (i.e.,  $E_6$  parallel to the [110] and [-110] directions) is decomposed in two principal directions (i.e.,  $E_1$  along the [100] direction and  $E_2$  along the [010] direction where  $E_1 = E_6 \cos \theta$  and  $E_2 = E_6 \sin \theta$  and induces in-plane polarizations only in the corresponding directions (i.e.,  $P_1$  and  $P_2$ , where  $P_1 = P_6 \cos \theta$  and  $P_2 = P_6 \sin \theta$ ). Then, from Eq. (4), the electric field  $E_6$  ( $\theta = 45^\circ$ ) can be expressed as

$$E_6 = (1/\sqrt{2})[\alpha(P_1 + P_2) + \beta(P_1^3 + P_2^3) + \gamma(P_1^5 + P_2^5) + \delta(P_1 P_2^2 + P_2 P_1^2) + 2G_{11}(x_1 P_1 + x_2 P_2) + 2G_{12} \times \{(x_2 + x_3)P_1 + (x_1 + x_3)P_2\} + G_{44}x_6(P_2 + P_1)]. \quad (5)$$

Since we can neglect the fifth-order or greater terms in  $P$  and we have  $P = \varepsilon E$  in the case of small electric fields  $E$ , we

have the following Curie-Weiss dependence of the dielectric constant  $\varepsilon$  above  $T_C$  where the spontaneous polarization is zero at zero electric field.<sup>15</sup> For a strain-free ferroelectric, we have

$$\partial E / \partial P = \alpha = (T - T_C) / C = 1 / \varepsilon. \quad (6)$$

From Eqs. (5) and (6), the phase-transition peak  $T_C^*$  for the applied electric field along the [110] or [-110] direction of the strained SrTiO<sub>3</sub> film can then be expressed as

$$T_C^* = T_C - \varepsilon_0 C \{G_{11}(x_1 + x_2) + G_{12}(x_1 + x_2 + 2x_3) + G_{44}x_6\}. \quad (7)$$

As we compare Eq. (7) with Eqs. (1) and (2), it can be expected that the phase transition will occur at a constant temperature regardless of the electric-field direction if the in-plane principal axial strains  $x_1$  and  $x_2$  are identical and the shear strain  $x_6$  is zero. Therefore, based on this theory, we can expect that there should be a nonzero shear strain in the film to explain the difference in the phase-transition peak position experimentally observed as in Fig. 6, and, in that case, the phase-transition peak will shift depending on the shear strain direction [i.e., positive shear strain causes  $T_C^*$  to increase and negative shear strain causes  $T_C^*$  to decrease because of the negative electrostriction coefficient  $G_{44}$  as in Eq. (7)]. At this point, the source of the shear strain in the film is not clearly understood but presumably results from a combination of a shear strain due to asymmetric biaxial elastic strains, whose difference between the in-plane strains  $x_1$  and  $x_2$  can be directly proportional to the magnitude of shear strain (i.e.,  $x_6 \sim |x_1 - x_2|$ ), and a shear strain due to the piezoelectric effect (i.e.,  $x_i = d_{ki} E_k$ ), whose coefficients  $d_{ki}$  are expected to be significant in this case (i.e., at room temperature). This is because the in-plane structure of the films is already asymmetric at room temperature and the phase-transition peak around which the piezoelectric effect should be significant is just below room temperature.<sup>20</sup> In addition to the existence of shear strain in the film, the polarization coupling  $P_1 P_2$  should also exist to explain the dependence of phase-transition peaks on the electric-field direction, as observed in Fig. 6. The polarization coupling causes a stress through an electrostriction effect ( $G_{44}$ ) [Eq. (3)], and the resultant stress ( $X_6 = G_{44} P_1 P_2$ ) is coupled with the shear strain  $x_6$  as a contribution to the total-energy function in Eq. (3), which will eventually be minimized, resulting in a shear strain relevant term in the form of  $G_{44} x_6$  in Eq. (7).

According to Eqs. (1) and (2), the theoretical phase-transition peaks for the applied electric field along [100] and [010] are expected to be 288 and 290 K, respectively, from the in-plane film strains ( $x_1$  and  $x_2$  are 0.0092 and 0.0094, respectively). These transition temperatures are comparable to the measured data along the corresponding directions [ $\sim 278$  and 280 K, respectively, in Fig. 6(a)]. Also, according to Eq. (7), the nonzero shear strain  $x_6$  in the film can be expected to be about  $-0.004$  so that the theoretical phase-transition peak for the electric field along the [110] or [-110] direction is 285 K, which is 5 K lower than that for the [010] direction (290 K) as we observed in the measured data [275 and 280 K in Fig. 6(a)]. A further study of the

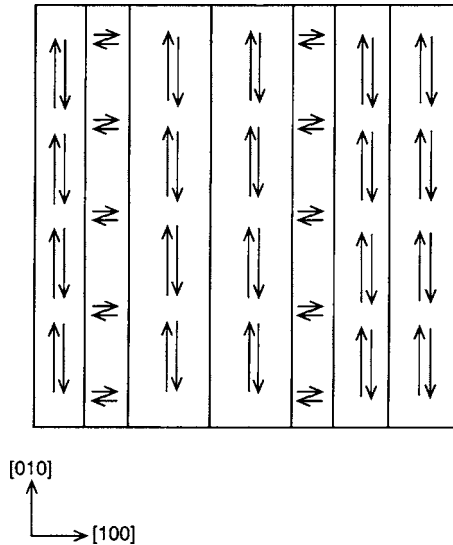


FIG. 7. A simple model of plausible polarization formation along the [010] and [100] directions of SrTiO<sub>3</sub> films when the small-signal electric field is applied along the [110] and [-110] directions.

shear strain is necessary to clarify its existence and magnitude in the films. Also, it is worth noting that the absolute value of the phase-transition temperatures in the theory may not have any significant meaning because it depends heavily on the electrostriction coefficients (i.e.,  $G_{11}$ ,  $G_{12}$ , and  $G_{44}$  and, subsequently,  $Q_{11}$ ,  $Q_{12}$ , and  $Q_{44}$  through  $G_{ij}=c_{ik}Q_{kj}$ ), which are not consistently and accurately known yet for the ferroelectric SrTiO<sub>3</sub> in literature.

In addition to the directional-dependent phase-transition peak, the dielectric constant of the SrTiO<sub>3</sub> films is observed to depend on the direction of the applied small-signal electric field (Fig. 5). To explain this observation, first, from Eqs. (1), (2), and (6) together with the precise known principal in-plane strains (i.e.,  $x_1$  and  $x_2$ ), we can have the theoretically expected dielectric constants (i.e., normalized dielectric constants) along the [100] and [010] directions as functions of the corresponding film strain when the small-signal electric field is applied along only the [100] and [010] directions of the films, respectively. Secondly, we can estimate the dielectric constant along the [110] or [-110] direction of the films from the theoretically expected dielectric constants along the [100] and [010] directions based on a simple model. Figure 7

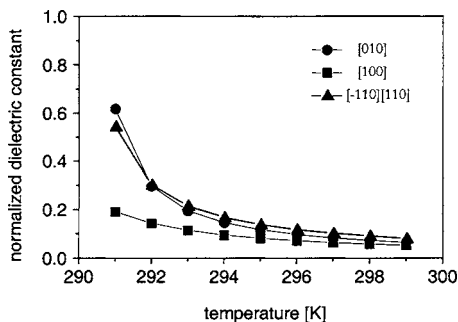


FIG. 8. Theoretical dielectric constant (normalized) of SrTiO<sub>3</sub> films in a paraelectric phase close to the phase-transition peak as a function of temperature and several measurement directions ([010], [100], [-110], and [110]).

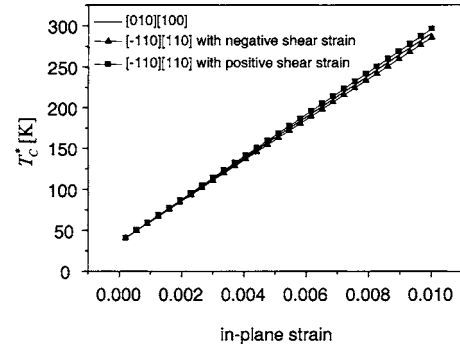


FIG. 9. Theoretical phase-transition peak as a function of film strains.

shows the simple model of plausible polarization formation only along the [010] and [100] directions when the electric field is applied in the direction of the [110] or [-110] SrTiO<sub>3</sub> films. As mentioned briefly in the previous section, we may expect larger polarization along the [010] direction of the films than that along the [100] direction when the small-signal electric field is applied along the [110] or [-110] direction of the films in the model. This is simply because of the larger strain along the [010] direction compared to the strain along the [100] direction ( $x_2 > x_1$ ). Figure 8 shows the theoretical dielectric constants (normalized) of the SrTiO<sub>3</sub> films in a paraelectric phase close to the phase-transition peak as functions of temperature and the measurement directions (i.e., large dielectric constant along the [010] direction compared to that along the [100] direction), which are consistent with the experimentally observed data [Figs. 5 and 6(a)], indicating that the film strains  $x_1$  and  $x_2$  have a significant effect on the dielectric constant. Also, Fig. 8 shows the dielectric constant along the [110] or [-110] direction of the films based on the theoretically expected dielectric constants along the [010] and [100] directions as  $\epsilon_6 = \epsilon_1 \cos 45^\circ + \epsilon_2 \sin 45^\circ$  by simply considering the contributions to the 45° direction from the dielectric constants in the principal axes  $\epsilon_1$  and  $\epsilon_2$ . The estimated dielectric constant along the [110] and [-110] directions based on the assumed model (i.e., only the polarizations  $P_1$  and  $P_2$  form with the electric field along the [110] or [-110] direction) is also consistent with the experimentally observed data [Fig. 6(a)], which are placed close to the dielectric constant along the [010] direction. Figure 9 shows the theoretical phase-transition peaks [Eqs. (1), (2), and (7)] as functions of film strains. As shown in the figure, we can expect that the shear-strained films (i.e., films on the electric field applied in the shear strain directions) show a little different (i.e., higher or lower) phase-transition temperature depending on the sign of the shear strain from that of the films on the electric field applied in the principal directions (i.e., [100] and [010]).

#### IV. SUMMARY

We have investigated the directional microwave tunable dielectric properties of strained SrTiO<sub>3</sub> films. A significant in-plane anisotropy in the dielectric constant and tuning is observed in the directional properties of the SrTiO<sub>3</sub> films. It was verified both experimentally and theoretically that the SrTiO<sub>3</sub> film in-plane principal strains  $x_1$  and  $x_2$  have a sig-

nificant effect on the relevant directional dielectric constant. Also, the shear strain  $x_6$  combined with the stress  $x_6$  which comes from the electrostriction effect through a coupling of the principal in-plane polarizations (i.e.,  $G_{44}P_1P_2$ ), can account for the experimentally observed shift in the phase-transition peak when the electric field is applied along the  $[110]$  or  $[-110]$  direction of the films.

<sup>1</sup>J. C. Slater, Phys. Rev. **78**, 748 (1950).

<sup>2</sup>P. W. Forsbergh, Jr., Phys. Rev. **93**, 686 (1954).

<sup>3</sup>G. A. Samara and A. A. Giardini, Phys. Rev. **140**, A954 (1965).

<sup>4</sup>J. H. Haeni *et al.*, Nature (London) **430**, 758 (2004).

<sup>5</sup>W. Chang, S. W. Kirchoefer, J. A. Bellotti, J. M. Pond, J. H. Haeni, and D. G. Schlom, J. Appl. Phys. **96**, 6629 (2004).

<sup>6</sup>N. A. Pertsev, A. K. Tagantsev, and N. Setter, Phys. Rev. B **61**, R825 (2000); **65**, 219901(E) (2002).

<sup>7</sup>V. Nagarajan *et al.*, Nat. Mater. **2**, 43 (2003).

<sup>8</sup>J. H. Haeni, C. D. Theis, and D. G. Schlom, J. Electroceram. **4**, 385 (2000).

<sup>9</sup>J. A. W. Dalziel, J. Chem. Soc. **1959**, 1993 (1959).

<sup>10</sup>JCPDS, Card No. 27-0204.

<sup>11</sup>J. H. Haeni *et al.*, J. Appl. Phys. (submitted).

<sup>12</sup>S. S. Gevorgian, T. Martinsson, P. I. J. Linner, and E. L. Kollberg, IEEE Trans. Microwave Theory Tech. **44**, 896 (1996).

<sup>13</sup>W. Chang, J. S. Horwitz, W. J. Kim, J. M. Pond, S. W. Kirchoefer, C. M. Gilmore, S. B. Qadri, and D. B. Chrisey, Integr. Ferroelectr. **24**, 257 (1999).

<sup>14</sup>J. M. Pond, S. W. Kirchoefer, W. Chang, J. S. Horwitz, and D. B. Chrisey, Integr. Ferroelectr. **22**, 837 (1998).

<sup>15</sup>A. F. Devonshire, Adv. Phys. **3**, 85 (1954).

<sup>16</sup>G. Schmidt and E. Hegenbarth, Phys. Status Solidi **3**, 329 (1963).

<sup>17</sup>K. A. Muller and H. Burkard, Phys. Rev. B **19**, 3593 (1979).

<sup>18</sup>T. Yamada, J. Appl. Phys. **43**, 328 (1972).

<sup>19</sup>The parameters used in this article:  $Q_{11}(\text{m}^4/\text{C}^2)=-0.066$ ,  $Q_{12}=0.015$ ,  $Q_{44}=-0.10$  (i.e., the relevant electrostriction coefficients have the opposite signs to the case of a Gibb's energy expression containing negatively signed electrostriction-related terms),  $C_{11}(10^{11} \text{ N/m}^2)=3.169$ ,  $C_{12}=1.026$ ,  $C_{44}=1.226$ ,  $T_C(\text{K})=35.5$ ,  $C(10^4 \text{ K})=8.0$ .

<sup>20</sup>D. E. Grupp and A. M. Goldman, Science **276**, 392 (1997).